Role of Internal Thermodynamics in Determining Hydrogen Tunneling in Enzyme-Catalyzed Hydrogen Transfer Reactions†

J. Rucker, Y. Cha,‡ T. Jonsson, K. L. Grant,§ and J. P. Klinman*

Department of Chemistry, University of California, Berkeley, California 94720

Received June 16, 1992; Revised Manuscript Received August 25, 1992

ABSTRACT: Previous investigations have indicated a role for hydrogen tunneling in the yeast alcohol dehydrogenase catalyzed oxidation of benzyl alcohol [Cha, Y., Murray, C. J., & Klinman, J. P. (1989) *Science 243*, 1325] and the bovine plasma amine oxidase catalyzed oxidation of benzylamine [Grant, K. L., & Klinman, J. P. (1989) *Biochemistry 28*, 6597]. In the present studies, values of protium to tritium and deuterium to tritium isotope effects and their temperature dependencies have been measured using ring-substituted substrates for yeast alcohol dehydrogenase and bovine plasma amine oxidase, revealing tunneling in each case. The results of these studies indicate that hydrogen tunneling is a general phenomenon and is not limited to enzyme reactions with degenerate energy levels for bound substrates and products. An analysis of internal thermodynamics in the yeast alcohol dehydrogenase reaction shows that tunneling occurs when $\Delta H°$ is endothermic and that the degree of tunneling appears to increase as $\Delta H°$ decreases toward zero.

Numerous examples exist in the literature documenting the importance of long distance electron tunneling in enzymatic processes [cf. Axup et al. (1988) and Boxer (1990)]. Although much larger than the electron, protium possesses a de Broglie wavelength which is similar to the expected dimension of the reaction coordinate in simple H transfer reactions (Bell, 1980). This property has led to the recognition that the behavior of the hydrogen is poised between classical and quantum mechanical behavior.

Recent studies from this laboratory have demonstrated that quantum effects do, in fact, contribute significantly to the room temperature, enzyme-catalyzed transfer of a hydride (Cha et al., 1989) and proton (Grant & Klinman, 1989). In the yeast alcohol dehydrogenase catalyzed hydride transfer reaction, measurement of protium to tritium (H/T) and deuterium to tritium (D/T) isotope effects has indicated significant breakdown from the Swain–Schaad relationship in the direction anticipated for tunneling (Cha et al., 1989). Evidence for tunneling in the proton-activated reaction catalyzed by bovine serum amine oxidase reaction has come from the observation of non-Arrhenius temperature dependencies, once again in the direction predicted for tunneling (Grant & Klinman, 1989). An unusual feature of the bovine plasma amine oxidase reaction was the failure to see a breakdown from Swain–Schaad relationships, despite the strong evidence for quantum effects. In a recent theoretical paper, it has been shown that deviations from Swain–Schaad relationships may vary considerably, depending on the relative importance of classical versus quantum behavior in a given reaction (Grant & Klinman, 1992).

Despite the unambiguous demonstration of hydrogen tunneling in several enzyme systems, many questions remain to be addressed. These include whether hydrogen tunneling is a ubiquitous phenomenon in enzyme-catalyzed H transfer reactions and, as a corollary, whether unique features of enzyme active sites will facilitate such quantum effects. Previous investigators have suggested that the catalytic strategy of enzymes may include a reduction in reaction barrier width (Hegazi et al., 1979; Bibbs et al., 1988; Borgis & Hynes, 1989; Bruno & Bialek, 1992) and an alteration in the internal thermodynamics for enzyme substrate and product interconversion to bring $\Delta G°$ closer toward zero (Nambiar et al., 1983; Burbaum et al., 1989). Theoretical and experimental considerations (Bell, 1980; de la Vega, 1982; Verhoeven et al., 1986; Wolfe et al., 1990; Kim et al., 1991; Bosch et al., 1992) indicate that both barrier widths and energy states for reactant versus product will influence the contribution of tunneling to a given H transfer process.

In this paper, we have begun to examine whether changes in internal thermodynamics can play a significant role in determining the degree to which quantum effects contribute to enzyme-catalyzed H transfer reactions. Using the yeast alcohol dehydrogenase and bovine plasma amine oxidase reactions as test cases, we have shown that modifications in substrate structure, relative to the parent compounds which were initially employed to demonstrate tunneling, preserve the phenomenon of tunneling. In the case of the yeast alcohol dehydrogenase catalyzed oxidation of ring substituted alcohols, significant changes in intrinsic isotope effects occur, despite the observation of identical rates. An examination of internal thermodynamics in this reaction has permitted a comparison of intrinsic isotope effects with the magnitude of $\Delta H°$ for the interconversion of bound alcohol and aldehyde. Two features emerge from these studies: first, that tunneling occurs when $\Delta H°$ internal is endothermic and second, that the degree of tunneling appears to increase as the energy gap between substrate and product diminishes.

EXPERIMENTAL PROCEDURES

Materials

Dimethyl sulfate, D_2O (99.9% and 99.996% D), ethyl alcohol-d_6 (99% D), BH_3/THF (1.37 M), phosphorus tri-

† This work supported by a grant to J.P.K. from the National Science Foundation (DMB 8911632), with additional support for Mr. Joseph Rucker from National Institutes of Health Molecular Biophysics Training Grant T32 GM08295.

* To whom correspondence should be addressed.

‡ Present address: Merck & Co., P.O. Box 2000 RY 123-22, Rahway, NJ 07065.

§ Present address: Genetics Institute, 87 Cambridge Park Dr., Cambridge, MA 02140.

0006-2960/92/0431-11489$03.00/0

bromide, 3,5-dinitrobenzoyl chloride, *p*-chlorobenzoylchloride, 4,4′-dimethoxybenzil, and $LiAlH_4$ were from Aldrich. Sodium borohydride, [ring-UL-^{14}C]*p*-hydroxybenzoic acid (8.8 or 12.0 mCi/mmol) and [ring-UL-^{14}C]*p*-chlorobenzoic acid (9.5 mCi/mmol) were from Sigma. BD_3/THF (1.0 M, 98% D) and $NaBD_4$ (99% D) were from Cambridge Isotope Laboratories, $LiAlD_4$ (99.1% D) and ethanol-free NAD^+ were from ICN, and [^{3}]$NaBH_4$ (0.5 Ci/0.25 mg; 50% ^{3}H) was from New England Nuclear. Sodium azide was from Fluka, hexadecyltri-*n*-butyl phosphonium bromide was from Alfa. All solvents were from Fischer and were used as obtained except for dimethyl ether and dimethylformamide, which were further dried over molecular sieves (5 Å), and tetrahydrofuran (THF)[1] and pyridine, which were distilled prior to use. Yeast alcohol dehydrogenase (YADH, lyophilized), aldehyde dehydrogenase, and NADH were from Boehringer. Horse liver alcohol dehydrogenase was from Sigma. Bovine serum amine oxidase (BSAO) was prepared to a specific activity of 0.24 unit/mg using a modification of the protocol outlined in Summers et al. (1979).

Synthesis of Radiolabeled Alcohols and Amines

C-14 p-Chlorobenzyl Alcohols. [1,1-$^1H_2$, ring-UL-^{14}C]- and [1,1-$^2H_2$, ring-UL-^{14}C]*p*-chlorobenzyl alcohols were synthesized by reduction of [ring-UL-^{14}C]*p*-chlorobenzoic acid (9.5 mCi/mmol) by $LiALH_4$ and $LiALD_4$, respectively, following protocols established for the production of protonated and deuterated [^{14}C]benzyl alcohols from [^{14}C]benzoic acid (Cha et al., 1989). Mass spectrometric analysis of the isotopic composition of deuterated product was unavailable, due to complexities introduced by the $^{35}Cl/^{37}Cl$ mass ratio. We therefore analyzed the isotopic composition of [1,1-$^2H_2$]-benzylalcohol, prepared in parallel with the *p*-chloro- substrate, estimating the deuterium content of [1,1-$^2H_2$]*p*-chlorobenzyl alcohol as 98.9%. Alcohols were purified by HPLC (reverse-phase C-18, eluted isocratically with 17.5% CH_3OH, 17.5% CH_3CN, 65% H_2O) and stored at −20 °C. Final specific activities were 2.3 μCi/μmol for the protonated compound and 1.6 μCi/μmol for the deuterated compound.

Tritiated p-Chlorobenzyl Alcohols. [1-^{1}H]- and [1-^{2}H]-*p*-chlorobenzaldehydes were prepared by the method of Brown et al. (1958a,b). In this synthesis, $LiAlH_4$ or $LiAlD_4$ is converted to tri-(*tert*-butoxy)aluminum hydride. This weaker reducing agent is then reacted with *p*-chlorobenzoyl chloride to form the corresponding *p*-chlorobenzaldehyde. As with *p*-chlorobenzyl alcohol, the isotopic composition of [1-^{2}H]*p*-chlorobenzaldehyde was obtained by analysis of the unsubstituted [1-^{2}H]benzaldehyde, synthesized in a parallel fashion. Mass spectrometric analysis of the benzaldehyde semicarbazone indicated a deuterium content of 99.6%. The H,T and D,T *p*-chlorobenzyl alcohols were synthesized by borotritide reduction of the [1-^{1}H]- and [1-^{2}H]aldehyde precursors, respectively. In a typical synthesis, [^{3}H]$NaBH_4$ (0.25 Ci/0.125 mg) was dissolved in 0.5 mL of a 5% NaOH solution and added to 70 mg (0.5 mmol) of aldehyde. This was refluxed gently for 3 h, followed by the addition of 20 mg (0.5 mmol) of $NaBH_4$ or $NaBD_4$. After being refluxed for 30 min, the mixture was allowed to stir overnight at room temperature. The reaction was quenched by the addition of 1 mL of water and the product extracted into ether. Tritiated alcohols were purified by HPLC (reverse-phase C-18, isocratic elution with 17.5% CH_3OH, 17.5% CH_3CN, 65% H_2O) and stored at −20 °C. Final specific activities were 11.8 μCi/μmol for both the protonated and deuterated compounds.

C-14 p-Methoxybenzyl Alcohols. A total of 125–250 μCi of [ring-UL-^{14}C]*p*-hydroxybenzoic acid and 0.25–0.5 mmol of unlabeled *p*-hydroxybenzoic acid were dissolved in 3–6 mL of anhydrous THF and added to 25-mL round bottom flasks which had been flame dried under N_2. Either BH_3/THF or BD_3/THF was added in a 6-fold excess while stirring on ice under N_2. The solution was refluxed gently for ca. 6 h or until complete by HPLC [reverse-phase C-18, eluted isocratically with 20% CH_3CN, 80% (0.1% acetate, pH 4.0)], at which point reaction was quenched by the slow addition of 0.2–1.0 mL of water. The resulting solution was transferred to a separatory funnel and sufficient ether added for an aqueous layer to separate out. This aqueous layer was further extracted with ether, the ether/THF extracts were combined, and the volume was reduced under a stream of N_2. Methylation was carried out by adding 0.75–2.0 mL of 10 M KOH and a 6-fold excess of dimethyl sulfate to the solutions of crude alcohol. These were stirred for 15–20 h at room temperature, until complete by HPLC (same condition as above). After addition of several milliliters of water, the methylated alcohols were extracted into ether. The products, [1,1-$^1H_2$, ring-UL-^{14}C]- and [1,1-$^2H_2$, ring-UL-^{14}C]*p*-methoxybenzyl alcohols, were purified on a silica column [Pasteur pipette size, eluted with CH_2Cl_2/ether (7:3)]. Final specific activities were 0.5 μCi/μmol for both protonated and deuterated products. Mass spectrometric analysis of a 3,5-dinitrobenzoyl chloride derivative of [1,1-$^2H_2$]*p*-methoxybenzyl alcohol, synthesized in parallel with [1,1-$^2H_2$, ring-UL-^{14}C]*p*-methoxybenzyl alcohol, indicated an H contamination of ca. 5%. However, the actual H content of radiolabeled alcohol has been estimated as 3%, using a kinetic analysis of radiolabeled amine derived by chemical derivatization of the alcohol precursor (cf. synthesis of C-14 *p*-methoxybenzylamine and Methods).

Tritiated p-Methoxybenzyl Alcohols. [1-^{1}H]- and [1-^{2}H]-*p*-methoxybenzaldehydes were prepared by a modification of the method of Burgstahler et al. (1972). By example, [1-^{2}H]-*p*-methoxybenzaldehyde was synthesized from 8.0 g (0.03 mol) of 4,4′-dimethoxybenzil which had been recrystallized from carbon tetrachloride. Glassware and four 1.0-g samples of KCN were dried overnight at 145 °C. The benzil was dissolved in 25 mL of freshly distilled dioxane, previously dried over 4-Å molecular sieves. Deuterium oxide (10 mL of 99.996% D) was transferred to the reaction flask under nitrogen. Every 2 min (for 8 min), 1.0 g of KCN was added. The solution was stirred overnight, cooled on ice for 5 min, transferred to a 250-mL separatory funnel to which 100 mL of ice-cold D_2O (99.9% D) was added, and washed twice with 50 mL of ether to extract *p*-methoxybenzaldehyde. The combined ether layers were then washed with 50 mL of 5% dipotassium carbonate in 99.9% D_2O, dried over sodium sulfate, and concentrated by rotary evaporation. Product *p*-methoxybenzaldehyde was purified by vacuum distillation and converted to the 2,4-dinitrophenylhydrazone derivative for analysis by mass spectrometry (99.8 ± 0.1% D). The H,T and D,T *p*-methoxybenzyl alcohol products were prepared by adding 0.12 g of the protonated or deuterated *p*-methoxybenzaldehyde to 10-mL round bottom flasks under argon. A 0.225-mL aliquot of a 5% NaOH solution, containing [^{3}H]$NaBH_4$ (0.25 Ci/0.125 mg), was added to each flask with vigorous stirring. After 3 h of reflux, 40 mg of $NaBH_4$ or 44 mg $NaBD_4$ was added. The reactions were stirred overnight and quenched with 2 mL

[1] Abbreviations: THF, tetrahydrofuran; YADH, yeast alcohol dehydrogenase; BSAO, bovine serum amine oxidase; HPLC, high-pressure liquid chromatography; TLC, thin-layer chromatography; TFA, trifluoroacetic acid.

of H_2O. Water and *p*-methoxybenzyl alcohols were lyophilized away from nonvolatile products and stored frozen until further use. Final specific activities of alcohols, after purification by HPLC, were 53 and 50 μCi/μmol for the protonated and deuterated compounds, respectively. Prior to kinetic assay, tritiated and C-14 *p*-methoxybenzyl alcohols were mixed in a ratio of radioactivity of ca. 10:1 and purified by HPLC (reverse-phase C-18, eluted isocratically with 20% CH_3CN, 80% H_2O).

C-14 p-Methoxybenzylamine. [1,1-$^1H_2$, ring-UL-^{14}C]- and [1,1-$^2H_2$, ring-UL-^{14}C]*p*-methoxybenzylamines were prepared from C-14 alcohol precursors (0.2 mmol and 0.4 mmol, respectively), which were dissolved in 15–20 mL of anhydrous ether and transferred to flame-dried round bottom flasks fitted with reflux condensers, septa, and stoppers. PBr_3 [0.1–0.25 mL (1–3 mmol)] was added with stirring under N_2. The resulting solutions were refluxed for ca. 6 h or until complete by TLC [dichloromethane/ether (7:3) or hexane/dichloromethane (1:1)], at which time reactions were quenched by the addition of water. *p*-Methoxybenzyl bromide was converted to the azide by removal of ether and use of either ethanol or dimethylformamide as solvent (Curtius & Ehrhart, 1922). A 4-fold excess of sodium azide was added and the solution stirred at 70–80 °C for 3 h. The resulting azide was reduced to amine at atmospheric pressure of hydrogen gas using 0.2 g of 5% Pd on activated charcoal as catalyst. When the azide was formed in dimethylformamide, it was first extracted into cold ether and reduced at 0 °C. Products were purified by HPLC (using conditions described under measurement of isotope effects with BSAO) and stored at −20 °C. Final specific activities for [1,1-$^1H_2$, ring-UL-^{14}C]- and [1,1-$^2H_2$, ring-UL-^{14}C]*p*-methoxybenzylamine were 0.3 and 0.5 μCi/μmol, respectively. As described under Methods, the H content of deuterated amine has been estimated as 3%.

Tritiated p-Methoxybenzylamine. H,T and D,T *p*-methoxybenzylamines were prepared from alcohol precursors (0.10 mmol and 0.09 mmol, respectively) which had been extracted into diethyl ether, dried over magnesium sulfate, and transferred to 25-mL flame-dried flasks under nitrogen. Nontritiated [1,1-$^1H_2$]- and [1,1-$^2H_2$]*p*-methoxybenzyl alcohols (0.35 mmol, 0.05 mL) were then added to the appropriate reaction mixtures. Phosphorus tribromide (0.20 mL, 2 mmol) was added to alcohols and allowed to react for 2 h. Each reaction was quenched with 0.5 mL of water, and the water layer was removed. The resulting *p*-methoxybenzyl bromides were converted to azides by the addition of 0.16 g of sodium azide, 0.05 g of hexadecyltri-*n*-butylphosphonium bromide, and 0.5 mL of water (Rolla, 1982). The solution was refluxed gently for 7 h and the water layer removed and discarded. The *p*-methoxybenzyl azides were reduced to amines with the addition of 0.12 g of sodium borohydride, 0.5 mL of water, and 0.12 g of toluene (Rolla, 1982). After refluxing overnight, one drop of 10 M potassium hydroxide was added. The toluene layer was removed, the remaining aqueous layer washed with ether, and the ether layers added to the toluene layers. Finally, the tritiated *p*-methoxybenzylamines were extracted from the mixtures of organic solvents into 1 M HCl and purified by HPLC [reverse-phase C-18, 8% CH_3CN, 92% (1% acetic acid, pH 4.0)]. The final specific activities were 12 and 10 μCi/μmol for [1,1-$^1H_2$,^3H]- and [1,1-$^2H_2$,^3H]*p*-methoxybenzylamines, respectively.

Synthesis of Deuterated Benzyl Alcohols and NADH.

The synthesis of [1,1-$^2H_2$]benzyl alcohols was carried out by reduction of the appropriate *para*-substituted benzoic acid with $LiAlD_4$. In a typical synthesis, 30 mmol of substituted benzoic acid was dissolved in 500 mL of ether and added dropwise to a solution of $LiAlD_4$ (2 g, 0.047 mol) in 90 mL of ether. Reaction was carried out under N_2 and allowed to proceed overnight (ca. 20 h). The reaction was quenched with 37 mL of D_2O and acidified with 200 mL of 5% H_2SO_4. The ether layer was removed and the aqueous layer extracted further with ether. The combined ether layers were dried over $MgSO_4$. Ether was removed by evaporation, and the alcohol products were purified by vacuum distillation. Phenylurethane derivatives were prepared by reacting phenyl isocyanate with the appropriately substituted alcohol using the method of Roberts et al. (1974). The phenylurethanes were analyzed by mass spectrometry for percent deuteration (benzyl alcohol, 97.8% D; *p*-methoxybenzyl alcohol, 98.9% D; *p*-chlorobenzyl alcohol, 98.9% D).

[4*R*-^2H]NADH (NADD) was prepared according to the method of Rafter and Colowick (1957) using ethanol-d_6 and ethanol-free NAD^+. Before each kinetic experiment, the NADD barium salt was converted to the sodium salt by a slight stoichiometric excess (by weight) of sodium sulfate. The resulting barium sulfate precipitate was removed by centrifugation. The concentration of NADD solutions was determined spectrophotometrically by absorbance at 340 nm (ϵ_{340} = 6.22 mM^{-1} cm^{-1}).

Methods

Measurement of H/T and D/T Kinetic Isotope Effects. Bovine Serum Amine Oxidase. All kinetic experiments were performed in 0.10 M pyrophosphate, pH 8.25, with 0.1–0.3 units of BSAO and 6500 units of catalase. The final concentration of *p*-methoxybenzylamine was ca. 1 mM and contained tritium and C-14 in the ratio of ca. 10. The temperature was kept constant to within 0.1 °C of the appropriate value in a Neslab or Thermomix water bath. The pH did change in the temperature range of the experiments (from pH 8.15 at 0 °C to 8.35 at 45 °C), but this change was assumed to have a negligible effect, since isotope effects on V_{max}/K_m for benzylamine are unchanged between pH 6 and 9 (Farnum et al., 1986). Samples were quenched with 2 mM $HgCl_2$ at appropriate time points and frozen on dry ice. HPLC analysis was carried out with a reverse-phase C-18 column, equilibrated with 0.2% TFA and 5% THF. A gradient of 0–42% methanol was run over 30 min at a flow rate of 1.0 mL/min, and 1-mL fractions were collected. Ecolite scintillation cocktail (8 mL) was added to each fraction, and the samples were analyzed with an LKB scintillation counter. The relative amount of tritium in water and C-14 in *p*-methoxybenzaldehyde was used to calculate the primary isotope effect, and the ratio of tritium to C-14 in *p*-methoxybenzaldehyde was used to obtain the secondary isotope effect. Isotope effects were calculated according to the general equation

$$k_L/k_T = \ln (1-f)/\ln (1-f[^3H/^{14}C]_f/[^3H/^{14}C]_\infty) \quad (1)$$

where L is H or D and f represents fractional conversion of reactants to products. Since $[^3H/^{14}C]_0$ was routinely equal to twice the value of $[^3H/^{14}C]_\infty$, the former was used to calculate the isotope effects.

Measurement of D/T isotope effects with substrates that are incompletely deuterated will lead to artifactual elevation of k_D/k_T. As discussed in detail by Grant and Klinman (1989), the H contamination can be corrected for, provided that the isotopic content of the substrate is known. As noted earlier, mass spectrometric analysis of a derivative of [1,1-$^2H_2$]*p*-

methoxybenzyl alcohol, synthesized in parallel with [1,1-$^2H_2$, ring-UL-^{14}C]*p*-methoxybenzyl alcohol, showed an H contamination of ca 5%. However, when the correction derived by Grant and Klinman was applied to the observed isotope effect, a sharp inverse trend was observed such that the isotope effect increased at late time points. This showed that the actual contamination of the deuterated [^{14}C]substrate was smaller than 5%. In order to estimate the correct contamination, we examined the percentage deviation (with sign) of each isotope effect [calculated from a modification of eq 1 (Grant & Klinman, 1989)] at a given fractional conversion from the average isotope effect for the entire experiment (3–8 points per experiment). This was carried out by assuming values of H contamination in the deuterated C-14-labeled substrate from 2–5%, and the results are shown in Figure 1 for 2%, 3%, and 4% corrections. The large number of data points represent all experiments carried out from 0 to 45 °C. For a correction of 3% (Figure 1B), the data display a random distribution of error, with a calculated least-squares slope very close to zero. By contrast, 2% and 4% corrections, Figure 1, panels A and C, show trends in opposite directions. This comparison indicates that the level of contamination in [1,1-$^2H_2$, ring-UL-^{14}C]*p*-methoxybenzylamine is 3% with an estimated uncertainty of ca. 0.2%. It should be pointed out that this type of analysis is only sound when sufficient data points have been collected to obtain a statistical distribution. We note that at early fractional conversions ($f < 0.2$), the experimental scatter is larger than at latter points, with lowest scatter at $f \sim 0.5$; these observations are in agreement with a previous prediction by Duggleby and Northrop (1989).

Yeast Alcohol Dehydrogenase. Isotope effects for the YADH-catalyzed reactions were determined according to Cha et al. (1989). All experiments were performed using 80 mM glycine, 100 mM semicarbazide, and 10 mM NAD^+ (final pH 8.5). Measurements with *p*-chlorobenzyl alcohol employed an overall alcohol concentration of 0.16 mM and a YADH concentration of 0.1–0.2 mg/mL. Experiments with *p*-methoxybenzyl alcohol employed an overall alcohol concentration of ca. 0.02–0.03 mM. For the H/T experiments with this substrate, it was found that incomplete trapping of product aldehyde with semicarbazide could artifactually lower the isotope effect. In order to compensate for this, YADH concentration was varied from 0.1 to 1.0 mg/mL and the measured primary isotope effect extrapolated linearly to zero enzyme (see Results). Experiments with D/T alcohols were found to be independent of changes in semicarbazide concentration at 0.2 mg/mL protein, and all D/T measurements were restricted to this low enzyme concentration.

In the course of reaction, samples were removed at appropriate time points, quenched with 1 mM $HgCl_2$, and frozen. For analysis, samples were thawed and reactants and products separated by HPLC (reverse-phase C-18, eluted isocratically with 13% CH_3OH, 13% CH_3CN, and 74% H_2O). Scintillation counting and data analysis were performed as discussed for BSAO-catalyzed reactions, using the appropriate correction for protium contamination in the D/T samples.

Determination of Thermodynamic Parameters for YADH-Catalyzed Oxidation of [1,1-$^2H_2$]Benzyl Alcohols and Reduction of Benzaldehydes by NADD. Benzyl alcohols and benzaldehydes were purified by vacuum distillation and stored at 4 °C. Concentrations of aldehyde solutions were determined either volumetrically or by enzymatic assay using horse liver alcohol dehydrogenase and excess NADH ($\Delta\epsilon_{340nm}$ = 6.22 mM^{-1} cm^{-1}). Alcohol solutions were assayed enzymatically with horse liver alcohol dehydrogenase, excess NAD^+, and

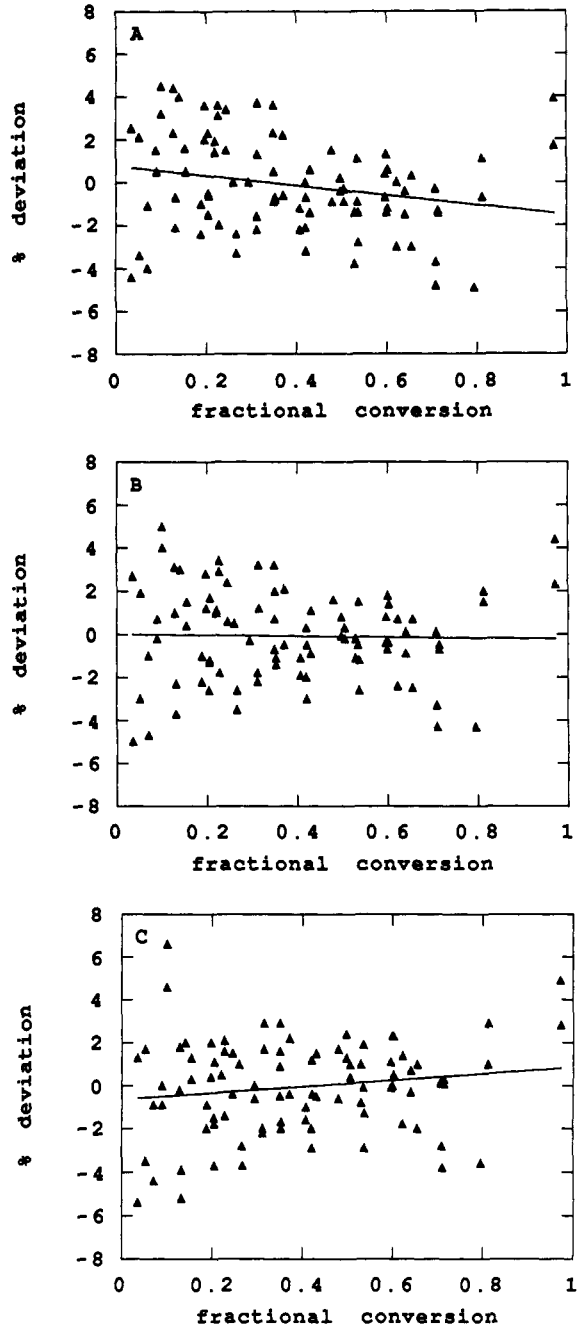

FIGURE 1: Deviation of D/T isotope effects as a function of fractional conversion from the average isotope effect per experiment (3–8 points per experiment). Data points represent all D/T isotope effects measured for the BSAO-catalyzed oxidation of *p*-methoxybenzylamine between 0 and 45 °C. Panels A–C represent 2%, 3%, and 4% protium contamination in deuterated *p*-methoxybenzylamine. Linear least-squares analysis indicated slopes of −1.92 (A), −0.03 (B), and 1.84 (C).

added aldehyde dehydrogenase ($\Delta\epsilon$ = 12.4 mM^{-1} cm^{-1}) to drive the reaction to completion. YADH concentrations were determined from absorbance at 280 nm ($A_{280,1\%}$ = 12.6). Enzyme kinetics were measured at pH 8.5 (40 mM potassium phosphate, 80 mM glycine) on a Cary 118 spectrophotometer in the temperature range of 5–40 ± 0.1 °C. Alcohol oxidation assays also contained 10 mM semicarbazide, to trap aldehyde and ensure the linearity of initial rate data. Initial rates were measured as a function of alcohol or aldehyde concentration using concentrations for cofactor maintained at several times K_m values. Initial rate data were fitted nonlinearly using Kaleidagraph on a Macintosh SE/30 computer. Values for k_{cat} were calculated by assuming four active sites per mol and

Table I: Value for k_H/k_T in the Oxidation of *p*-Methoxybenzylamine by BSAO at 25 °C, pH 8.25[a]

primary isotope effect	secondary isotope effect
21.7 ± 1.0	1.09 ± 0.03
18.7 ± 0.7	1.11 ± 0.02
av 20.2 ± 1.9[b]	1.10 ± 0.03[b]

[a] Each experiment consisted of 3–5 time points. [b] Average and standard deviation of all time points.

were normalized to a specific activity of 100 units/mg with respect to ethanol oxidation at 25 °C [1.0 M ethanol, 4 mM NAD^+, pH 8.5 buffer (Klinman, 1972)]. Enzyme activity was approximately constant over a day. Plots of ln k_{cat} versus $1/T$ were analyzed by linear least-squares regression to obtain E_a and $T\Delta S^\ddagger$. $\Delta H^\ddagger$ was obtained from E_a using the expression $\Delta H^\ddagger = E_a - RT$.

Analogous to studies with BSAO, the pH of the buffer was found to vary from ca. 8.35 (5 °C) to 8.65 (40 °C). Previous studies of pH dependencies with YADH indicate a pK_a value of 8.25 (Klinman, 1975), with the temperature dependence of the enzymic pK_a unknown. It is possible that the enzymic pK_a changes with temperature in a manner analogous to the buffer, precluding any correction for small changes in pH over the experimental temperature. Alternatively, if the enzymic pK_a is either temperature insensitive or changes in a direction opposite to the buffer, trends could appear in the final values of $\Delta H^\ddagger$ and $T\Delta S^\ddagger$. We therefore modeled the effect of a temperature-independent pK_a for YADH on final values for $\Delta H^\ddagger$, finding that $\Delta H^\ddagger$ for alcohol oxidation would decrease by ca. 4 kJ/mol and $\Delta H^\ddagger$ for *p*-methoxybenzaldehyde reduction would increase by ca. 8 kJ/mol. These changes would lead to final values of $\Delta H°$ which are smaller than the values in Table VI but which give the same overall trend of $\Delta\Delta H° = 8$ kJ/mol in proceeding from *p*-methoxy to *p*-chloro substrates.

RESULTS

Analysis of Tunneling in the Bovine Serum Amine Oxidase Catalyzed Oxidation of p-Methoxybenzylamine. Previous studies of BSAO were focused on the analysis of H/T and D/T isotope effects in the enzyme-catalyzed oxidation of benzylamine. Despite the very large magnitude of the H/T primary isotope effect and the evidence for a single rate-limiting H transfer step, the relationship between H/T and D/T isotope effects failed to indicate $(k_D/k_T)^{3.26} < (k_H/k_T)$, the benchmark of tunneling in the YADH reaction (Cha et al., 1989). By contrast, examination of primary isotope effects as a function of temperature revealed large deviations from Arrhenius behavior with pre-Arrhenius factors, A_D/A_T and A_H/A_T, significantly less than unity. Given the evidence for a single rate-limiting H transfer step, the deviation of A_L/A_T provided clear evidence for tunneling. Of particular significance was the finding that $A_D/A_T < 1$. Since D/T isotope effects were expected to be completely free of complications arising from kinetic complexity, $A_D/A_T < 1$ confirms the conclusion reached from H/T isotope effects and implies significant deuterium as well as hydrogen tunneling (Grant & Klinman, 1989).

Our studies of BSAO have now been extended to include primary and secondary H/T and D/T isotope effects using a ring-substituted benzylamine, *p*-methoxybenzylamine. The magnitude of H/T isotope effects at 25 °C is given in Table I. The primary value of 20.2 is reduced from a value of 35.2 previously measured with benzylamine (Grant & Klinman, 1989), suggesting that the H transfer step is not fully rate limiting with *p*-methoxybenzylamine. The measurement of the primary D/T isotope effect with *p*-methoxybenzylamine at 25 °C indicates a value of 2.86 (Table II) for an exponential relationship between D/T and H/T of 2.86. The reduction of this value from a semiclassical value of 3.26 is consistent with the view that H transfer is only partially rate limiting at 25 °C (Cha et al., 1989). The secondary H/T isotope effect for *p*-methoxybenzylamine at 25 °C is 1.10 (Table I), for comparison to a previously measured value of 1.195 for benzylamine itself (Grant & Klinman, 1989).

Previous stopped flow measurements of the BSAO reaction have indicated similar, large deuterium isotope effects for a series of substrates (Hartmann & Klinman, 1991). It is therefore reasonable to assume that intrinsic isotope effects for *p*-methoxybenzylamine oxidation will be close to values

Table II: Values for k_D/k_T in the Oxidation of *p*-Methoxybenzylamine by BSAO as a Function of Temperature, pH 8.25[a]

temp (°C)	primary isotope effect	secondary isotope effect
0	3.33 ± 0.09	1.052 ± 0.010
0	3.32 ± 0.16	1.028 ± 0.025
15	2.94 ± 0.06	1.046 ± 0.023
15	3.07 ± 0.13	1.045 ± 0.011
25	2.80 ± 0.05	1.033 ± 0.018
25	2.92 ± 0.05	1.038 ± 0.032
35	2.62 ± 0.03	1.016 ± 0.013
45	2.55 ± 0.06	
45	2.53 ± 0.02	1.040 ± 0.023
45	2.57 ± 0.05	1.037 ± 0.021

[a] Each experiment consisted of 3–8 time points.

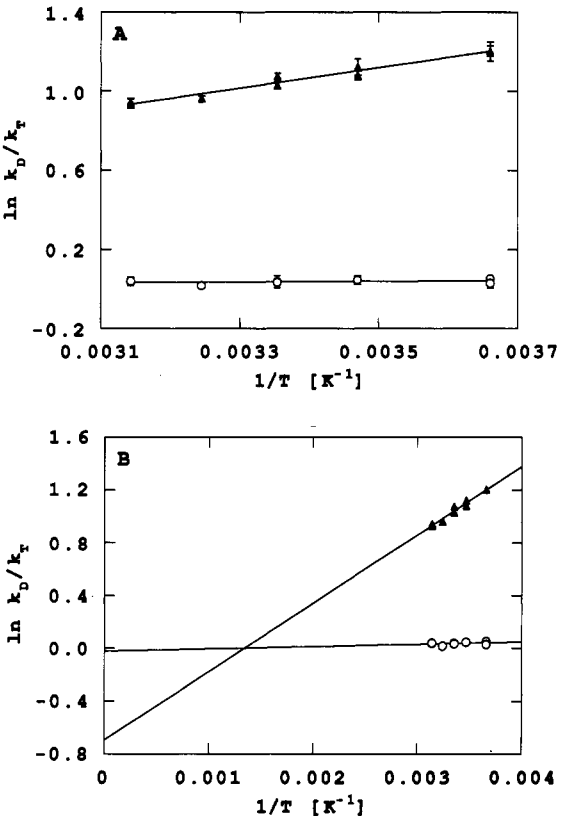

FIGURE 2: Temperature dependence of D/T isotope effects for the BSAO-catalyzed oxidation of *p*-methoxybenzylamine at pH 8.25 (Table II). Panel A represents the experimental temperature range, and panel B shows the extrapolation of data to $T = \infty$. (▲) Primary isotope effects; (○) secondary isotope effects.

Table III: Isotope Effects on Arrhenius Prefactors for the Oxidation of Deuterated, Tritiated *p*-Methoxybenzylamine and Benzylamine by BSAO

	A_D/A_T		$E_a(T) - E_a(D)$ (kJ/mol)	
	p-methoxy[a]	*p*-H[b]	*p*-methoxy[a]	*p*-H[b]
primary isotope effect	0.50 ± 0.05	0.51 ± 0.10	4.31 ± 0.26	4.51 ± 0.48
secondary isotope effect	0.98 ± 0.06	1.02 ± 0.06	0.14 ± 0.16	0.07 ± 0.14

[a] This study. [b] Grant and Klinman (1989).

seen with unsubstituted benzylamine. Using the available primary tritium isotope effect data for *p*-H (Grant & Klinman, 1989) and *p*-methoxybenzylamine (Table I), together with the equation $^T(k_{cat}/K_m) = (^Tk + X)/(1 + X)$ [where $^T(k_{cat}/K_m)$ is the observed isotope effect, ^Tk is the intrinsic isotope effect, and X is the ratio of rate constants for substrate oxidation to substrate release from enzyme], X is calculated to be 0.78 for *p*-methoxybenzylamine oxidation. This result, which indicates approximately equal rates for substrate oxidation and release from enzyme, could generate anomalous temperature dependencies in the absence of tunneling, and hence no effort was made to measure H/T isotope effects as a function of temperature.

Turning to D/T isotope effects, these are more effective tools for detecting tunneling for several reasons. First, the commitment X will be reduced by the magnitude of the primary deuterium isotope effect, which, given a value of k_H/k_D of ca. 12, is estimated to be only 0.07. This is near to zero, allowing close to full expression of the intrinsic D/T isotope effect. Second, examination of Table II indicates a primary D/T isotope effect at 25 °C of 2.86 ± 0.05, which is almost within experimental error of the previously measured value of 3.07 ± 0.07 for unsubstituted benzylamine (Grant & Klinman, 1989). We therefore pursued the temperature dependence of both primary and secondary D/T isotope effects for *p*-methoxybenzylamine oxidation in the temperature range of 0–45 °C (Table II). The data in Table II are represented in a graphical form in Figure 2, where panel A shows the experimental temperature range and panel B the full temperature range permitting extrapolation to infinite temperature. Arrhenius parameters obtained from the intercepts of Figure 2B are summarized in Table III, together with previously measured values for benzylamine. It can be seen that the values for A_D/A_T and $E_a(T) - E_a(D)$ derived from primary isotope effects for *p*-methoxybenzylamine lie outside the semiclassical range and are almost identical to values previously measured for benzylamine. As previously discussed by Grant and Klinman (1989), this behavior provides strong evidence for deuterium tunneling in substrate oxidation. Arrhenius parameters derived from secondary isotope effects with *p*-methoxybenzylamine lie within the semiclassical range, once again analogous to benzylamine. In no instance have abnormalities indicative of coupled motion between the primary and secondary hydrogen positions been observed in the BSAO reaction. This behavior contrasts with the YADH reaction, where anomalous secondary isotope effects reflect a propagation of tunneling from the primary to secondary position as a result of coupled motion [cf. below and Cha et al. (1989)].

Analysis of Tunneling in the Yeast Alcohol Dehydrogenase Catalyzed Oxidation of p-Chloro- and p-Methoxybenzyl Alcohol. Early studies of structure reactivity correlations in the YADH reaction indicated a large increase in rate for the reduction of ring-substituted benzaldehydes with electron-withdrawing substituents (Klinman, 1972), together with little or no effect of ring substituent on benzyl alcohol oxidation (Klinman, 1976). In the case of the unsubstituted substrate benzyl alcohol, the internal equilibrium constant for the interconversion of alcohol and aldehyde [$K_{eq(internal)} = k_f/k_r$] was found to be close to unity, with ring-donating substituents leading to an increase in $K_{eq(internal)}$ and ring-withdrawing substituents leading to a decrease in $K_{eq(internal)}$.

Table IV: Values for k_H/k_T and k_D/k_T in the Oxidation of *p*-Chlorobenzyl Alcohol by Yeast Alcohol Dehydrogenase, pH 8.5

temp (°C)	$k_D/k_{T(obs)}$[a]	$k_H/k_{T(calc)}$[b]	$k_H/k_{T(obs)}$[a]	exponent[c]
	Primary Isotope Effects			
0	1.71 ± 0.02	5.75 ± 0.22	7.49 ± 0.29	3.75 ± 0.11
25	1.59 ± 0.03	4.53 ± 0.28	6.59 ± 0.13	4.06 ± 0.17
	Secondary Isotope Effects			
0	1.04 ± 0.01	1.14 ± 0.04	1.38 ± 0.01	8.21 ± 2.0
25	1.03 ± 0.01	1.10 ± 0.03	1.34 ± 0.01	9.90 ± 4.2

[a] Observed isotope effects. Values are the average of 2–3 experiments, comprised of 4–6 time points. [b] Calculated from $k_D/k_{T(obs)}$, assuming classical behavior, $[k_D/k_{T(obs)}]^{3.26} = k_H/k_{T(calc)}$. [c] Exponent relating $k_D/k_{T(obs)}$ and $k_H/k_{T(obs)}$: $[k_D/k_{T(obs)}]^{Exp} = k_H/k_{T(obs)}$.

We have now pursued primary and secondary H/T and D/T isotope effects in the YADH-catalyzed oxidation of *p*-chloro- and *p*-methoxybenzyl alcohol for comparison to previous results with the parent benzyl alcohol. Data for *p*-chlorobenzyl alcohol at 0 and 25 °C are summarized in Table IV. As previously discussed (Saunders, 1985; Cha et al., 1989), the relationship between H/T and D/T isotope effects is expected to be $(k_D/k_T)^{3.26} = (k_H/k_T)$ in the absence of tunneling versus $(k_D/k_T)^{3.26} < (k_H/k_T)$ in the presence of tunneling. The values of k_H/k_T calculated from $(k_D/k_T)^{3.26}$ have been included in Table IV as $(k_H/k_T)_{calc}$. In every instance, $(k_H/k_T)_{calc}$ falls significantly below $(k_H/k_T)_{obs}$. Although propagation of errors increases the uncertainty in $(k_H/k_T)_{calc}$ relative to $(k_D/k_T)_{obs}$, the values of $(k_H/k_T)_{calc}$ fall well outside the error range in $(k_H/k_T)_{obs}$. The exponents which will accommodate the experimental data, $(k_D/k_T)^{Exp} = (k_H/k_T)$, are 3.75 (0 °C) and 4.06 (25 °C) for primary isotope effects and 8.21 (0 °C) and 9.90 (25 °C) for secondary isotope effects.

Two features emerge from the data in Table IV. First, the values of the exponents relating H/T and D/T isotope effects increase with increasing temperature. This trend is in a direction opposite from that expected for tunneling, suggesting that the kinetic significance of the H transfer step decreases slightly with decreasing temperature. As noted earlier, kinetic complexity leads to $(k_D/k_T)^{3.26} > (k_H/k_T)$ and, hence, tends to obscure the phenomenon of tunneling (Cha et al., 1989). Previous studies of the temperature dependence of H/T isotope effects in the YADH oxidation of benzyl alcohol indicated classical Arrhenius intercepts, despite the clear cut evidence for tunneling from exponential relationships (Cha et al., 1989). In light of the present data with *p*-chlorobenzyl alcohol, we attribute our failure to observe $A_H/A_T < 1$ in the YADH reaction to increasing kinetic complexity at reduced temperatures. The second major conclusion to emerge from the measured isotope effects with *p*-chlorobenzyl alcohol is the inflation of exponents from their semiclassical limit of 3.26–3.34. At 25 °C, the exponents seen with *p*-chlorobenzyl alcohol

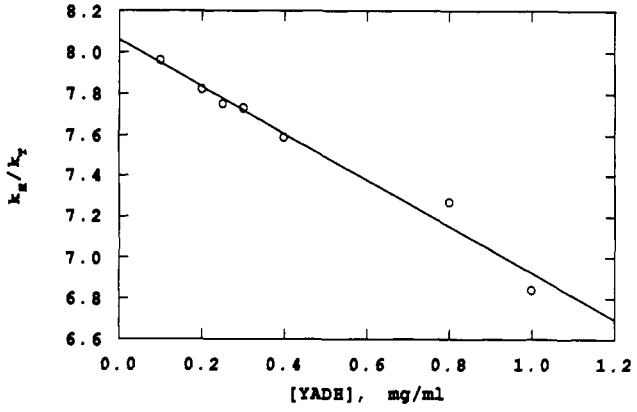

FIGURE 3: Dependence of the primary H/T isotope effect for *p*-methoxybenzyl alcohol oxidation by YADH (25 °C, pH 8.5) on enzyme concentration.

are similar to those seen previously with benzyl alcohol, 4.06 versus 3.58 for primary isotope effects and 9.90 versus 10.2 for secondary isotope effects. This indicates that tunneling plays as significant a role in *p*-chlorobenzyl alcohol oxidation as was previously concluded for benzyl alcohol oxidation.

In light of the appearance of small commitments with decreasing temperature for *p*-chlorobenzyl alcohol (Table IV), comparison of k_H/k_T to k_D/k_T for *p*-methoxybenzyl alcohol oxidation was restricted to 25 °C. Initial studies indicated more variability in the final magnitude of the H/T isotope effect than had been seen with either benzyl alcohol or *p*-chlorobenzyl alcohol. As described under Methods, YADH isotope effects are measured by coupling product aldehydes to semicarbazide to prevent reversal of the enzymatic reaction. Literature studies of semicarbazide addition to benzaldehydes indicate a significant reduction in this rate for electron-releasing substituents (Anderson & Jencks, 1960). The critical factor in the YADH reaction is the ratio of enzyme concentration to trapping reagent. Initially, we chose to maintain the concentration of semicarbazide at 100 mM and to vary the enzyme concentration between 0.1 and 1.0 mg/mL. Results of such studies are shown in Figure 3, where the primary H/T isotope effect can be seen to increase from ca. 7 to a limiting value of ca. 8. The secondary H/T isotope effects varied in a random manner and were simply averaged over the entire enzyme concentration range. The absence of a trend in the secondary effects is consistent with their small size and the similarity of measured kinetic isotope effects to the equilibrium limit [$K_{eq,H}/K_{eq,T} = 1.34$ (Welsh et al., 1980)]. As expected from the slower rate for enzymic interconversion of deuterated substrates, D/T isotope effects were found to insensitive to changes in semicarbazide concentration at 0.2 mg/mL enzyme, and all experiments were performed at this enzyme level.

Final values of H/T and D/T isotope effects at 25 °C for *p*-methoxybenzyl alcohol are given in Table V. One feature that is immediately apparent is that the exponents relating both primary and secondary H/T and D/T effects are less than 3.26. This is attributed to the presence of some kinetic complexity with the *p*-methoxybenzyl alcohol, although we cannot rule out an especially high degree of tunneling with this substrate as the origin of the observed exponents [cf. Grant and Klinman (1992)]. We note that the magnitude of the secondary D/T isotope effect for *p*-methoxybenzyl alcohol is much larger than values observed with the other two substrates and is at the equilibrium limit of 1.09 ± 0.02 (Welsh et al., 1980). The latter result was completely unexpected, leading us to consider whether artifacts in the method of synthesis or incomplete deuteration of ^{14}C-labeled *p*-methoxybenzyl alcohol could be the source of an inflated isotope effect. Both of these possibilities were ruled out by (i) the observation of identical isotope effects using separate batches of deuterated, ^{14}C-labeled alcohol synthesized by different researchers over a period of several years and (ii) the availability of a highly accurate method for determination of the percent contamination of the deuterated substrate by protium (cf. Methods).

Internal Thermodynamics in the Yeast Alcohol Dehydrogenase Reaction. As previously demonstrated (Klinman, 1976), the internal equilibrium constant, $K_{eq(internal)}$, for the interconversion of the E·NAD$^+$·alcohol and E·NADH·aldehyde complexes in the YADH reaction at 25 °C can be estimated in a fairly straightforward manner from measured values for k_{cat} in the directions of alcohol oxidation (k_f) and aldehyde reduction (k_r), $K_{eq(internal)} = k_f/k_r$. Measurement of kinetic parameters with deuterated alcohol and NADH, respectively, assures that measured rate constants reflect the hydride transfer step exclusively.

In the present study, we wished to estimate the values of internal equilibrium constants as a function of temperature for *p*-chloro, *p*-H, and *p*-methoxybenzyl alcohols, with the goal of obtaining $\Delta H°$ and $\Delta S°$ for the interconversion of bound reactants and products. Rate constants for deuterated alcohol oxidation have been measured in the temperature range of 0–45 °C, leading to the Arrhenius plots in Figure 4. These data provide values of $\Delta H^‡$ and $T\Delta S^‡$ for alcohol oxidation, summarized in Table VI. Efforts to obtain similar parameters in the direction of aldehyde reduction led to experimental difficulties, a result of high K_m values for substituted benzaldehydes, their limited solubility in water, and a temperature dependence on K_m. Taken together, these properties precluded aldehyde saturation across the experimental temperature range with the *p*-H and *p*-chlorobenzyl alcohols. Given the lower K_m and greater solubility of *p*-methoxybenzyl alcohol, it was possible to estimate $\Delta H^‡$ and $T\Delta S^‡$ (Figure 5 and Table VI).

Focusing on the *p*-methoxybenzyl alcohol data, an unexpected feature is the large magnitude of $T\Delta S^‡$ describing k_{cat} values for both alcohol oxidation and aldehyde reduction. Although the $T\Delta S°$ describing $\Delta G°$ reflects a partial cancellation of the contribution of $T\Delta S^‡$ to k_f and k_r, the magnitude of $T\Delta S°$ is still substantial. We considered the possibility that changing the substituent in the para position of benzyl alcohol might have a significantly greater effect on $\Delta H°$ than $T\Delta S°$. In the event that $T\Delta S°$ were only weakly

Table V: Values for k_H/k_T and k_D/k_T in the Oxidation of *p*-Methoxybenzyl Alcohol by Yeast Alcohol Dehydrogenase, pH 8.5, 25 °C

	$k_D/k_{T(obs)}$[a]	$k_H/k_{T(calc)}$[b]	$k_H/k_{T(obs)}$[a]	exponent[c]
primary isotope effect	1.94 ± 0.06	8.67 ± 0.87	8.06 ± 0.04	3.13 ● 0.15
secondary isotope effect	1.12 ± 0.02	1.45 ± 0.08	1.34 ± 0.04	2.78 ± 0.82

[a] Observed isotope effects. $k_D/k_{T(obs)}$ is the average of five experiments, consisting of 4–6 time points. The primary $k_H/k_{T(obs)}$ was obtained by extrapolation to zero enzyme concentration (Figure 3). The secondary $k_H/k_{T(obs)}$ was averaged over the entire enzyme concentration rage of 0.1–1.0 mg/mL (see text). [b] Calculated from $k_D/k_{T(obs)}$ assuming classical behavior, $[k_D/k_{T(obs)}]^{3.26} = k_H/k_T(calc)$. [c] Exponent relating $k_D/k_{T(obs)}$ and $k_H/k_{T(obs)}$: $[k_D/k_{T(obs)}]^{Exp} = k_H/k_{T(obs)}$.

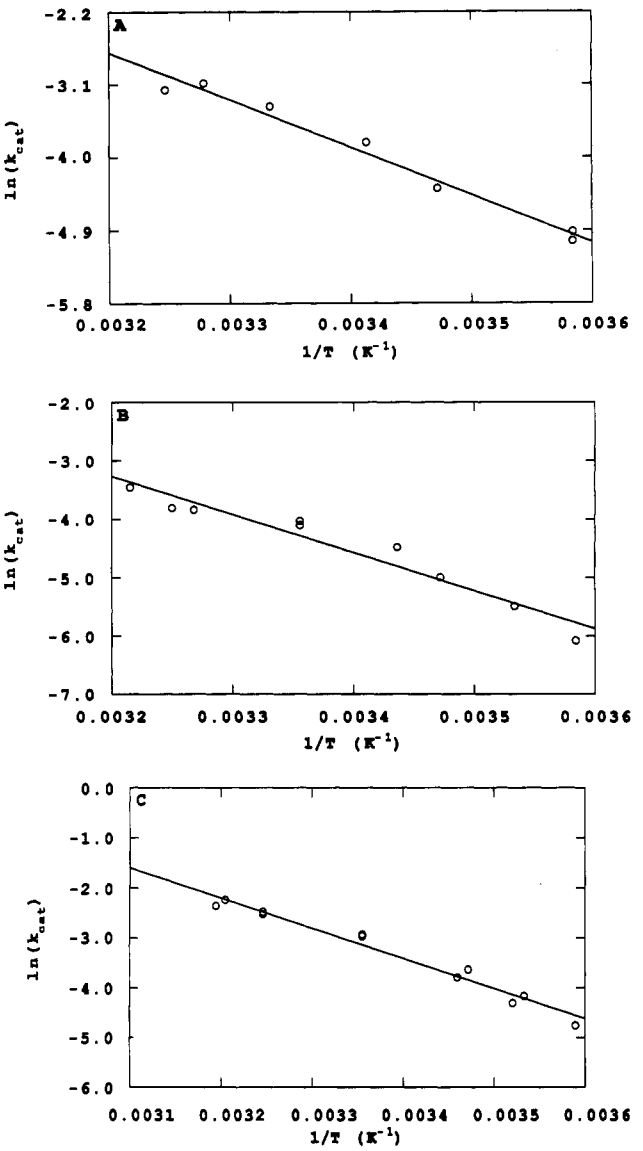

FIGURE 4: Arrhenius plots for the temperature dependence of k_{cat} for the oxidation of [1,1-$^2H_2$]benzyl alcohol by NAD^+, catalyzed by YADH. *p*-Methoxybenzyl alcohol (A), benzyl alcohol (B), and *p*-chlorobenzyl alcohol (C).

dependent on ring structure, the available value of $T\Delta S°$ with *p*-methoxybenzyl alcohol could be used in conjunction with $\Delta G°$ values to estimate $\Delta H°$ for the other aromatic substrates in the series. Given the independence of $T\Delta S^‡$ on substrate structure in the direction of alcohol oxidation, this required demonstrating that $T\Delta S^‡$ is also insensitive to structure in the direction of aldehyde reduction.

The above assumption was tested with *p*-methylbenzaldehyde, a substrate whose greater solubility permitted an estimate of k_{cat} across the experimental temperature range, providing $\Delta H^‡ = 34.3 \pm 5.8$ kJ/mol and $T\Delta S^‡ = 44.8 \pm 9.2$ kJ/mol. The uncertainty in the activation parameters for *p*-methylbenzaldehyde is considerably greater than seen with *p*-methoxybenzaldehyde (Table VI), a result of the lowered solubility of the *p*-methyl compound and the difficulty in reaching K_m concentrations at all temperatures. Nonetheless, the value of $T\Delta S^‡$ for *p*-methylbenzaldehyde lies within experimental error of the value for *p*-methoxybenzaldehyde. We have therefore used the value of $T\Delta S° = 15.4$ kJ/mol to calculate $\Delta H°$ for the *p*-H and *p*-chloro substrates (Table VI).

Table VI: Thermodynamic Parameters for *para*-Substituted Benzyl Alcohols and Benzaldehydes Interconverted by YADH, pH 8.5[a]

	substituent		
parameter	*p*-methoxy	*p*-H	*p*-chloro
$\Delta H^‡$ (alcohol)[b]	46.4 ± 2.9	51.9 ± 5.0	47.7 ± 2.5
$T\Delta S^‡$ (alcohol)[b]	−35.6 ± 2.9	−31.8 ± 3.8	−33.0 ± 2.1
$\Delta G^‡$ (alcohol)	82.0 ± 4.2	83.7 ± 6.3	82.0 ± 3.3
$\Delta H^‡$ (aldehyde)[c]	33.5 ± 2.9	NA[d]	NA[d]
$T\Delta S^‡$ (aldehyde)[c]	−51.0 ± 6.3	NA[d]	NA[d]
$\Delta G^‡$ (aldehyde)	84.5 ± 5.8	NA[d]	NA[d]
$\Delta H°$	12.9 ± 4.1[e]	15.6[g]	21.2[g]
$T\Delta S°$	15.4 ± 6.9[e]	15.4	15.4
$\Delta G°$	−6.9[f] (−2.5 ± 7.2[e])	0.20[f]	5.8[f]

[a] All values in kJ/mol. [b] $\Delta H^‡$ and $\Delta S^‡$ from Arrhenius plots, Figure 4; $T = 25$ °C. [c] $\Delta H^‡$ and $\Delta S^‡$ from Arrhenius plot, Figure 5; $T = 25$ °C. [d] Not available experimentally (see text). [e] Calculated from $\Delta H^‡$, $T\Delta S^‡$, and $\Delta G^‡$ for alcohol vs aldehydes. In each case, the size of the error envelopes is a result of taking the difference of two large numbers. [f] From Klinman (1976), obtained by comparison of experimental k_{cat} values for alcohol oxidation and aldehyde reduction at 25 °C. [g] Calculated from $\Delta G°$ values (Klinman, 1976), using $T\Delta S°$ for the *p*-methoxy substituent (see text). Although the range of $\Delta\Delta H°$ will vary with $T\Delta S°$, the direction of the trend among substrates is independent of the absolute value of $T\Delta S°$.

DISCUSSION

Earlier studies of both yeast alcohol dehydrogenase and bovine serum amine oxidase had indicated a significant tunneling contribution to the enzyme-catalyzed oxidation of benzyl alcohol (Cha et al., 1989) and benzylamine (Grant & Klinman, 1989), respectively. This ability to observe H tunneling suggested that the substrates under investigation may have been fortuitously chosen to yield degenerate energy levels for E·S to E·P interconversion [since this condition is expected to optimize tunneling (Bell, 1980; De la Vega, 1982)]. In the present work, we have examined the effect of perturbations in substrate structure on the phenomenon of tunneling in each case.

Bovine Plasma Amine Oxidase. A recently completed investigation of structure reactivity correlations in the bovine plasma amine oxidase has indicated a linear correlation between the rate of hydrogen abstraction and benzylamine ring substituent, $\rho = 1.47 \pm 0.27$, attributed to a proton abstraction mechanism for the topa quinone catalyzed oxidation of substrate (Hartmann & Klinman, 1991):

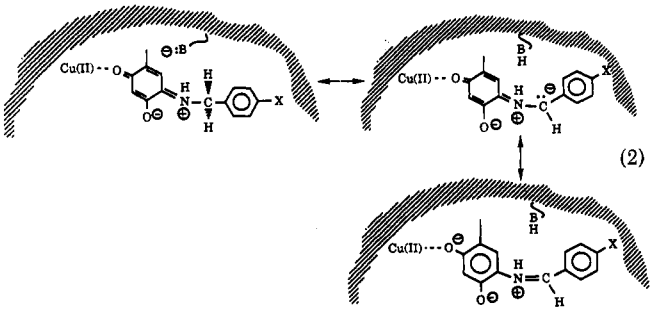

Unexpectedly, the rate for *p*-methoxybenzylamine oxidation was found to be significantly faster than that of other ring-donating substituents, with a rate of oxidation similar to that for the trifluoromethyl substituent (both of which occur ca. 10-fold faster than the parent compound benzylamine).

A possible explanation for this observation is that the *p*-methoxy substituent undergoes protonation at the enzyme active site, converting an electron-donating into a electron-withdrawing substituent. As summarized in Table I, the

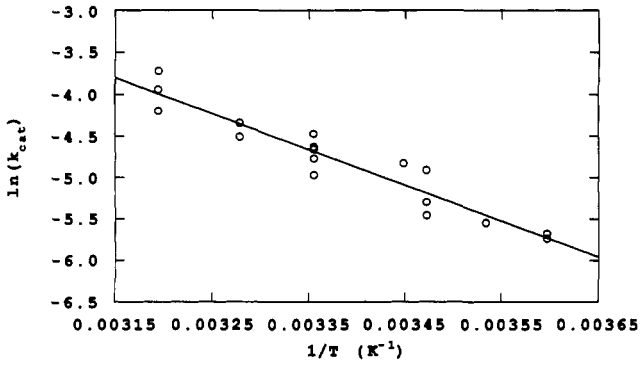

FIGURE 5: Arrhenius plot for the temperature dependence of k_{cat} for the reduction of *p*-methoxybenzaldehyde by [1*R*-^{2}H]NADH catalyzed by YADH.

magnitude of the primary tritium isotope effect for *p*-methoxybenzylamine at 25 °C is only 20.2, reduced from a value of 35 previously observed with benzylamine (Grant & Klinman, 1989). This is consistent with a faster rate for hydrogen abstraction from *p*-methoxybenzylamine than benzylamine, such that k_{cat}/K_m has become partially rate limited by the substrate-binding step. As described under Results, we can estimate the ratio of rate constants for substrate oxidation to substrate release to be 0.78 for protonated substrate versus only 0.07 for deuterated substrate. As expected for a large reduction in the commitment to catalysis for deuterated *p*-methoxybenzylamine, its primary D/T isotope effect at 25 °C (Table II) is almost within experimental error of the previously measured value for benzylamine [3.07 ± 0.07 (Grant & Klinman, 1989)].

Given the very small commitment to catalysis with deuterated *p*-methoxybenzylamine, measured D/T isotope effects will approximate intrinsic values. We have examined the magnitude of primary and secondary D/T isotope effects as a function of temperature (Figure 2), finding an intercept for the primary D/T Arrhenius plot significantly less than unity, A_D/A_T = 0.50 ± 0.05 (Table III). This result, which is analogous to previous studies with benzylamine (Grant & Klinman, 1989), implicates significant tunneling for both *p*-methoxybenzylamine and benzylamine.

A full analysis of tunneling among a series of enzymatic substrates requires knowledge of internal equilibrium constants as well as rates. In the course of our studies of structure reactivity correlations in the BSAO reaction (Hartmann & Klinman, 1989), pre-steady-state kinetics with *p*-acetylbenzylamine indicated a reversible process for the H transfer step, characterized by a forward rate constant of 82 s^{-1} and $K_{eq(internal)}$ = 66 (Hartmann & Klinman, 1989). More recent single-turnover experiments with *p*-hydroxybenzylamine (Hartmann and Klinman, unpublished results) indicate a forward rate constant of 16 s^{-1} and $K_{eq(internal)}$ = 15. This comparison indicates that changes in substrate structure give rise to perturbations in $K_{eq(internal)}$ (4-fold) which are similar to changes in rate constants (5-fold). Unfortunately, values for $K_{eq(internal)}$ with *p*-H- and *p*-methoxybenzylamines have not been experimentally accessible. However, the difference in forward rate constants for these substrates (2.6 and 18 s^{-1} for *p*-H- and *p*-methoxybenzylamine, respectively) suggests that their internal equilibrium constants will vary in a manner similar to *p*-hydroxy- and *p*-acetylbenzylamine. Thus, given rate differences between *p*-H- and *p*-methoxybenzylamines of 7-fold, a similar disparity in $K_{eq(internal)}$ can be anticipated, indicating that tunneling will not be restricted to substrates for which the energy states of bound reactants and products are degenerate. A more quantitative analysis of the interdependence of tunneling and internal thermodynamics has been possible in the context of the yeast alcohol dehydrogenase reaction.

Table VII: Intrinsic k_D/k_T Isotope Effects for the Oxidation of Benzyl Alcohols by YADH, 25 °C, pH 8.5

	substituent		
	p-methoxy[a]	*p*-H[b]	*p*-chloro[c]
primary isotope effect	1.94 ± 0.06	1.73 ± 0.02	1.59 ± 0.03
secondary isotope effect	1.12 ± 0.02	1.03 ± 0.01	1.03 ± 0.01

[a] From Table V. [b] From Cha et al. (1989). [c] From Table IV.

Yeast Alcohol Dehydrogenase. In the present investigation, tritium isotope effects for the oxidation of two ring-substituted benzyl alcohols have been measured (Tables IV and V) for comparison to benzyl alcohol (Cha et al., 1989). Given the availability of both H/T and D/T isotope effects, it has been possible to examine their exponential relationships as probes of tunneling. Although this approach leads to the conclusion of significant tunneling for *p*-chlorobenzyl alcohol (Table IV), it breaks down in the case of the *p*-methoxy substrate (Table V). The observation of exponential relationships less than 3.26 in the latter case is attributed to some kinetic complexity, with the rate of either alcohol binding or aldehyde dissociation from ternary complex contributing to k_{cat}/K_m.

As discussed above for the bovine serum amine oxidase reaction, D/T isotope effects will provide intrinsic values when the H transfer step can be shown to be close to fully rate limiting. Since this property has been demonstrated for the YADH-catalyzed interconversion of aromatic substrates (Klinman, 1972; Klinman, 1976), we present the D/T isotope effects in Table VII as intrinsic values. An unexpected trend emerges from this comparison, in which both primary and secondary D/T effects increase in a regular fashion in proceeding from *p*-chloro- to *p*-methoxybenzyl alcohol. This trend occurs, despite the fact that the rates of alcohol oxidation are the same among the three substrates (Klinman, 1976). In the direction of aldehyde reduction, the reaction driving force is *p*-Cl > *p*-H > *p*-CH_3O (Klinman, 1972) predicting the earliest transition state for the *p*-chlorobenzaldehyde and, hence, the largest isotope effects with this substrate.[2] From a classical view of reaction dynamics, changes in isotope effects are interpreted in terms of changes in transition-state structure, which reflect changes in substrate reactivity. Clearly, other factors must be operative in the YADH reaction.

One of the advantages of the YADH reaction is the possibility of studying the reaction in both directions, providing values for $K_{eq(internal)}$, $\Delta G°$, $\Delta H°$, and $T\Delta S°$ (Table VI). Although the ability to interpret $\Delta H°$ and $T\Delta S°$ as enthalpic changes for bond making/breaking steps and entropic changes for accompanying structural reorganizations, respectively, is complex for solution reactions (Jencks, 1987), we reasoned that $\Delta H°$ would be a closer approximation of internal energetics than $\Delta G°$ for the YADH reaction. This is borne out in two ways. First, the data presented under Results and in Table VI suggest that $T\Delta S°$ will be constant among a series of alcohols and aldehydes, with the result that changes in $\Delta G°$ with substrate will reflect changes in the $\Delta H°$ term. Second, the trend in isotope effects (Table VII) correlates with $\Delta H°$ (Table VI), which predicts the largest isotope effect with the *p*-methoxy substrate. This is in contrast to $\Delta G°$,

[2] Given the evidence for an alcohol-like transition state [cf. Cha et al. (1989)], both primary and secondary isotope effects are expected to increase as the transition state becomes more aldehyde-like.

Scheme I: Energy Diagrams for the Interconversion of E·S ($E{\cdot}NAD^+{\cdot}RCH_2O^-$) and E·P ($E{\cdot}NADH{\cdot}RHC{=}O$) Catalyzed by YADH, Illustrating the Greater Region Available for Tunneling (Shaded Areas) as the Energetics of Reactants and Products Become Matched

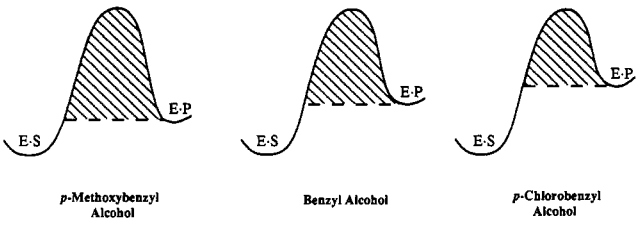

which predicts a peak in isotope effect for the unsubstituted substrate.

As shown in eq 3, the hydride transfer from enzyme-bound

(3)

alcohol to NAD^+ is believed to occur from the oxyanion of alcohol, formed by a pre-equilibrium deprotonation of alcohol. An unresolved issue in the alcohol dehydrogenase reaction is the pK_a of bound alcohols, with estimates ranging from 7 to 10 [cf. Klinman (1981), Maret and Makinen (1991), and Pettersson (1987)]. Given a pH of 8.5 for the present experiments, a low pK_a for bound alcohol would indicate that the thermodynamic parameters in Table VI refer to the interconversion of the species shown in eq 3. Alternatively, if the pK_a of bound alcohol exceeds 8.5, the measured thermodynamic parameters will reflect both an unfavorable ionization of alcohol and the subsequent hydride transfer:

$$pK_a < 8.5: \quad E{\cdot}NAD^+ \cdot RCH_2O^- \overset{K_{eq(internal)}}{\rightleftharpoons} E \cdot NADH\ RCHO$$

$$pK_a > 8.5: \quad E{\cdot}NAD^+ \cdot RCH_2OH \overset{K_1,\ H^+}{\rightleftharpoons} E \cdot NAD^+ \cdot RCH_2O^- \overset{K_2}{\rightleftharpoons} ENADH \cdot RCHO$$

$$K_{eq(internal)} = K_1K_2$$

(4)

It is expected that electron-withdrawing substituents will favor substrate deprotonation such that the energy of the anion will be closer to the energy of the protonated alcohol for *p*-chlorobenzyl alcohol than *p*-methoxybenzyl alcohol. Thus, correction for the contribution of K_1 to $K_{eq(internal)}$ would be greatest for the *p*-methoxy substituent and least for the *p*-chloro substituent. This effect can only increase the range of $\Delta H°$ values for hydride transfer among ring-substituted alcohols, such that the magnitude of $\Delta\Delta H°$ would exceed that of 8.0 kJ/mol summarized in Table VI.

Overall, the data in Table VII indicate (i) that tunneling occurs in the YADH reaction when $\Delta H°$ is endothermic and (ii) that the tunneling probability increases as $\Delta H°$ goes toward zero. This type of behavior is, in fact, predicted from models which treat tunneling as a correction to the rate near the top of the reaction barrier, e.g., the Bell correction (Bell, 1980). As illustrated for our series of ring-substituted substrates of YADH (Scheme I), the reduction of the overall $\Delta H°$ toward zero has the effect of increasing the region under the curve which is available for tunneling [shown as the shaded areas (Bell, 1980)]. A more recent and rigorous treatment of H-transfer reaction is variational transition-state theory (Truhlar & Garrett, 1980; Truhlar & Gordon, 1990), which reveals corner cutting (tunneling) by both H and D near the top of the energy barrier. An important feature of variational transition-state theory is that H and D tunnel at different configurations, with D tunneling requiring a closer approach between reactants than H tunneling. This theory has been very successful in modeling both rates and isotope effects in model hydride transfer reactions in solution (Kreevoy & Lee, 1989; Kim et al., 1991), showing that tunneling is the predominant pathway and that it occurs 4–8 kJ/mol beneath the top of the reaction barrier.

Currently, efforts are underway to model the YADH reaction using both the Bell correction and variational transition-state theory. The latter approach, while more rigorous and difficult, will provide a potential energy surface for the YADH reaction. It will be extremely insightful to see which parameters are critical in providing a match between experimental data and theory. In particular, it will be interesting to see if small changes in distance between reactants can effect significant changes in isotope effects. This type of correlation, which has been observed in model calculations, indicates that tunneling increases with increasing distance between reactants (Kim et al., 1991). Such a result, which at first glance may appear counterintuitive, reflects the different distance dependencies for passing over the top of the barrier (classical behavior) versus corner cutting (tunneling). In light of such studies, we cannot rigorously exclude a change in distance between reacting atoms as a cause of trends in tunneling and isotope effects in the YADH reaction. However, the demonstrated correlation between D/T isotope effects (Table VII) and $\Delta H°$ (Table VI) argues for a role of internal thermodynamics in modulating tunneling in YADH, as well as other enzyme H-transfer reactions.

REFERENCES

Anderson, B. M., & Jencks, W. P. (1960) *J. Am. Chem. Soc. 82*, 1773.

Axup, A. W., Albin, M., Mayo, S. L., Crutchley, R. J., & Gray, H. B. (1988) *J. Am. Chem. Soc. 110*, 435, and references therein.

Bell, R. P. (1980) *The Tunnel Effect in Chemistry*, Chapman & Hall, New York.

Bibbs, J. A., Denuth, H.-U., Huskey, W. P., Mordy, C. W., & Schowen, R. L. (1988) *J. Mol. Catal. 47*, 187.

Borgis, D., & Hynes, J. T. (1989) in *The Enzyme Catalysis Process* (Copper, A., Houben, J. L., & Chien, L. C., Eds.) p 293, Plenum Press, New York.

Bosch, E., Moreno, M., & Lluch, J. M. (1992) *J. Am. Chem. Soc. 114*, 2072.

Boxer, S. G. (1990) *Annu. Rev. Biophys. Biophys. Chem. 19*, 100.

Brown, H. C., & McFarlin, R. F. (1958a) *J. Am. Chem. Soc. 80*, 5372.

Brown, H. C., & Subba Rao, B. C. (1958b) *J. Am. Chem. Soc. 80*, 5377.

Bruno, W., & Bialek, W. S. (1992) *Biophys. J. 63*, 689.

Burbaum, J. J., Raines, R. T., Albery, W. J., & Knowles, J. R. (1989) *Biochemistry 28*, 9293.

Burgstahler, A. W., Walker, D. E., Jr., Kuebvice, J. P., & Schowen, R. L. (1972) *J. Org. Chem. 37*, 1272.

Cha, Y., Murray, C. J., & Klinman, J. P. (1989) *Science 243*, 1325.

Curtius, T., & Erhart, G. (1922) *Ber. Dtsch. Chem. Ges. 55*, 1559.

de la Vega, J. R. (1982) *Acc. Chem. Res. 15*, 185.

Duggleby, R. G., & Northrop, D. B. (1989) *Bioorg. Chem. 17*, 177.

Farnum, M., Palcic, M., & Klinman, J. P. (1986) *Biochemistry 25*, 1898.

Grant, K. L., & Klinman, J. P. (1989) *Biochemistry 28*, 6597.
Grant, K. L., & Klinman, J. P. (1992) *Bioorg. Chem. 20*, 1.
Hartmann, C., & Klinman, J. P. (1991) *Biochemistry 30*, 4605.
Hegazi, M. F., Borchardt, P. T., & Schowen, R. L. (1979) *J. Am. Chem. Soc. 101*, 4395.
Jencks, W. P. (1987) *Cold Spring Harbor Symposia on Quantitative Biology*, Vol. L11, p 65, Cold Spring Harbor Press, Cold Spring Harbor, NY.
Kim, Y., Truhlar, D. G., & Kreevoy, M. M. (1991) *J. Am. Chem. Soc. 113*, 7837.
Klinman, J. P. (1972) *J. Biol. Chem. 247*, 7977.
Klinman, J. P. (1975) *J. Biol. Chem. 250*, 2569.
Klinman, J. P. (1976) *Biochemistry 15*, 2018.
Klinman, J. P. (1981) *CRC Crit. Rev. Biochem. 10*, 39.
Kreevoy, M. M., & Lee, I.-S. H. (1989) *Z. Naturforsch. A 44*, 418.
Nambiar, K. P., Stauffer, D. M., Kolodziej, P. A., & Benner, S. A. (1983) *J. Am. Chem. Soc. 105*, 5886.
Pettersson, G. (1987) *CRC Crit. Rev. Biochem. 21*, 349.
Rafter, G. W., & Colowick, S. P. (1957) *Methods Enzymol. 3*, 887.
Roberts, R. M., Gilbert, J. C., Rodewald, L. B., & Wingrove, A. S. (1974) in *An Introduction to Modern Experimental Organic Chemistry*, 2nd ed., p 446, Holt, Rinehart & Winston, Inc., New York.
Rodgers, J., Femec, D. A., & Schowen, R. C. (1982) *J. Am. Chem. Soc. 104*, 3263.
Rolla, F. (1982) *J. Org. Chem. 47*, 4327.
Saunders, W. H. (1985) *J. Am. Chem. Soc. 107*, 164.
Summers, M. C., Markovic, R., & Klinman, J. P. (1979) *Biochemistry 18*, 1969.
Truhlar, D. G., & Garrett, B. C. (1980) *Acc. Chem. Res. 13*, 440.
Truhlar, D. G., & Gordon, M. S. (1990) *Science 249*, 491.
Verhoeven, J. W., Koomen, G. J., & van der Kerk, S. M. (1986) *Recl. Trav. Chim. Pays-Bas 105*, 343.
Welsh, K. M., Creighton, D. J., & Klinman, J. P. (1980) *Biochemistry 19*, 2005.
Wolfe, S., Hoz, S., Kim, C.-K., & Yang, K. (1990) *J. Am. Chem. Soc. 112*, 4186.